



An "Endless" Route to Cyclic Polymers

Christopher W. Bielawski, *et al.*

Science **297**, 2041 (2002);

DOI: 10.1126/science.1075401

The following resources related to this article are available online at www.sciencemag.org (this information is current as of September 17, 2007):

Updated information and services, including high-resolution figures, can be found in the online version of this article at:

<http://www.sciencemag.org/cgi/content/full/297/5589/2041>

A list of selected additional articles on the Science Web sites **related to this article** can be found at:

<http://www.sciencemag.org/cgi/content/full/297/5589/2041#related-content>

This article has been **cited by** 66 article(s) on the ISI Web of Science.

This article has been **cited by** 1 articles hosted by HighWire Press; see:

<http://www.sciencemag.org/cgi/content/full/297/5589/2041#otherarticles>

This article appears in the following **subject collections**:

Chemistry

<http://www.sciencemag.org/cgi/collection/chemistry>

Information about obtaining **reprints** of this article or about obtaining **permission to reproduce this article** in whole or in part can be found at:

<http://www.sciencemag.org/about/permissions.dtl>

region of greatest and most recent uplift. Indeed, the locus of maximum and most recent uplift that we infer on the basis of thermochronometric data also coincides with the center of the positive Bouguer gravity anomaly beneath Fiordland (Fig. 1).

Assuming a 1 cm/year convergence rate [e.g., (3)], about ~1 to 2 km of dynamic support or bedrock uplift within 2 to 4 My of the initiation of subduction is predicted (1). The amount of uplift on a continental margin might be larger than 1 to 2 km because erosion in response to uplift of the overriding plate may lead to further isostatic uplift. On the basis of the range of crustal and mantle densities typical for Fiordland crust as well as the fraction of the gravity anomaly due to dynamic support (5), the upper crust of central and northern Fiordland must have been thinned by ~7 km to maintain the current average surface elevation and positive gravity anomaly beneath Fiordland. This is similar to the estimate of thinning which we infer based on thermochronometric data from regions coinciding with the gravity anomaly (~4 to 7 km in the Doubtful Sound region), implying that the denudation that we detect and the present day dynamic support of Fiordland have a common origin (SOM Text).

Thermochronologic data from Fiordland record evidence for uplift and exhumation that is temporally related to the inception of subduction offshore of Fiordland. Geodynamic models predict a northward progression in the locus of uplift as subduction propagates northward, which appears to be consistent with denudation tracked thermochronometrically in southern and central-northern Fiordland at ~11 and ~5 Ma, respectively. Although factors like the curved geometry of the Fiordland coast (Fig. 1) and the morphology of the subducted slab below Fiordland (3, 20–23) may play a role in determining how uplift propagates across Fiordland (SOM Text), the agreement between the amount of denudation we observe across Fiordland with the amount of crustal thinning required by the amount of dynamic uplift evident in the gravity signature of the region suggests that these processes are linked. This correlation, coupled with the temporal agreement between enhanced denudation and the onset of subduction offshore of Fiordland implies that we have dated the initiation of subduction along this segment of the Australian-Pacific plate boundary using thermochronometric means (24).

References and Notes

1. J. Toth, M. Gurnis, *J. Geophys. Res.* **103**, 18053 (1998).
2. A. I. Shemenda, *J. Geophys. Res.* **97**, 11097 (1992).
3. F. J. Davey, E. G. C. Smith, *Geophys. J. R. Astron. Soc.* **72**, 23 (1983).
4. J. Y. Collot et al., *Eos* **76**, 1 (1995).
5. M. Broadbent, F. J. Davey, R. I. Walcott, *Technical Report No. 124* (New Zealand Department of Sci-

- tific and Industrial Research, Lower Hutt, New Zealand, 1978).
6. R. I. Walcott, *Rev. Geophys.* **36**, 1 (1998).
7. C. DeMets, R. G. Gordon, D. F. Argus, S. Stein, *Geophys. J. Int.* **101**, 425 (1990).
8. H. Anderson, T. Webb, J. Jackson, *Geophys. J. Int.* **115**, 1032 (1993).
9. I. M. Turnbull et al., *Technical Report No. 1* (Institute of Geological and Nuclear Sciences, Lower Hutt, New Zealand, 1993).
10. C. M. Ward, *Am. Mineral.* **69**, 531 (1984).
11. P. J. J. Kamp, K. A. Hegarty, *Geophys. J. R. Astron. Soc.* **96**, 33 (1989).
12. D. G. Bishop, *Spec. Publ. Int. Assoc. Sedimentol.* **12**, 69 (1991).
13. C. DeMets, R. G. Gordon, D. F. Argus, S. Stein, *Geophys. Res. Lett.* **18**, 2191 (1994).
14. P. F. Green et al., *Chem. Geol.* **79**, 155 (1989).
15. K. A. Farley, *J. Geophys. Res.* **105**, 2903 (2000).
16. A. J. W. Gleadow, I. R. Duddy, P. F. Green, J. F. Lovering, *Contrib. Mineral. Petrol.* **94**, 405 (1986).
17. Materials and Methods are available as SOM on Science Online

18. D. G. Bishop, N. Z. *J. Geol. Geophys.* **28**, 243 (1985).
19. C. M. Ward, *J. R. Soc. N. Z.* **18**, 1 (1988).
20. D. A. Christoffel, W. J. M. Van der Linden, *Ant. Res. Series* **19**, 235 (1972).
21. J.-F. Lebrun, G. D. Karner, J.-Y. Collot, *J. Geophys. Res.* **103**, 7293 (1998).
22. ———, J. Delteil, *Tectonics* **19**, 688 (2000).
23. D. Eberhart-Phillips, M. Reyners, *Geophys. J. Int.* **146**, 731 (2001).
24. Supported by NSF grant EAR-0003558 to M.A.H. and M.G. We thank J. Braun for discussions and J. Braun and T. Ehlers for access to software used in the modeling. Comments from three anonymous reviewers greatly improved the manuscript.

Supporting Online Material

www.sciencemag.org/cgi/content/full/297/5589/2038/DC1

Methods and Materials

SOM Text

Tables S1 to S8

Figs. S1 to S3

21 June 2002; accepted 12 August 2002

An "Endless" Route to Cyclic Polymers

Christopher W. Bielawski, Diego Benitez, Robert H. Grubbs*

A new synthetic route to cyclic polymers has been developed in which the ends of growing polymer chains remain attached to a metal complex throughout the entire polymerization process. The approach eliminates the need for linear polymeric precursors and high dilution, drawbacks of traditional macrocyclization strategies, and it effectively removes the barrier to producing large quantities of pure cyclic material. Ultimately, the strategy offers facile access to a unique macromolecular scaffold that may be used to meet the increasing demand of new applications for commercial polymers. As a demonstration of its potential utility, cyclic polyethylenes were prepared and found to exhibit a variety of physical properties that were distinguishable from their linear analogs.

Produced at a rate of 40 million tons per year, polyethylene remains one of the most valuable synthetic polymers in the world. It is now used in products ranging from grocery bags and milk containers to high-performance fibers and medical devices. Its versatility stems from our ability to tune the material's crystallinity, mechanical strength, and thermal stability by altering the architecture of the individual polymer chains (1). However, the rising number of applications for polyethylene require its material properties to be broadened even further. Though most efforts have been focused on synthesizing polyethylene with increasing structural complexity, here we were interested in exploring whether unique properties could be obtained through the simplest of topological modifications; for example, tying the ends of a linear precursor together to form a cyclic polymer conceptually varies the structure only minimally. However, the additional physical con-

straints imposed on such a cyclic polymer would not only restrict conformational freedom but also reduce its overall dimensions and, therefore, may lead to unusual or unexpected properties.

Although cyclic polymers have been synthesized previously, access to high molecular weight material (MW > 100 kD), which is often required for many polymers to show their characteristic physical properties, is exceedingly challenging (2). The typical synthetic route involves intramolecular macrocyclization of linear precursors at extremely low concentrations. Alternatively, the balance between linear and cyclic products that occurs for many polymerizations (e.g., polycondensations, metathesis polymerizations, etc.) may be shifted to maximize formation of cyclic product (which again generally involves using low concentrations). Incomplete cyclizations or undesired side reactions are common for both approaches; therefore, elaborate purification procedures are often required to remove the acyclic contaminants (3). Furthermore, many monomers, including ethylene, are not amenable to these types of polymerizations. As a result, there are very few reported examples of cyclic polyeth-

Arnold and Mabel Beckman Laboratories of Chemical Synthesis, Division of Chemistry and Chemical Engineering, California Institute of Technology, Pasadena, CA 91125, USA.

*To whom correspondence should be addressed.

ylenes, especially in the high molecular weight ($>10^4$ dalton) regime, and thus the physical properties and potential applications of this material remain largely unexplored (4, 5).

The drawbacks of the cyclization techniques cited above could be circumvented by eliminating the linear intermediates. This would require an "endless" polymerization process where cyclic monomers are linked together in such a fashion that the overall circularity of the system is not compromised during polymer growth (6). Lastly, it is preferable that the resulting cyclic polymer is easily isolable and stable and that it possesses no evidence of the polymerization process (i.e., no incorporation of undesired functional groups). Herein, we demonstrate these requirements can be met using ring-opening metathesis polymerization (ROMP) (7) in conjunction with cyclic Ru-based catalysts (8).

The cyclic Ru complex $L(PCy_3)Cl_2Ru=CHR$ (noted here as **A**) was prepared in a manner similar to a previously reported procedure (9). Addition of **A** to *cis*-cyclooctene (monomer) in the bulk or in solution at 40°C initiated the polymerization (Fig. 1). After a predetermined amount of monomer was polymerized, the resulting macrocyclic complex (noted here as **B**) underwent intramolecular chain transfer to yield cyclic polymer and **A** (10). After the polymerization reached completion (~12 hours), the addition of excess acetone or methanol caused polymer to precipitate, which was then isolated by filtration. No additional purification steps were necessary (11). A variety of polymers with number-averaged molecular weights (M_n 's) up to 1200 kD were prepared by varying the initial monomer/catalyst ratio and/or the initial monomer concentration (12). In all cases, the polydispersity indices (PDIs) of the resulting polymers were around 2.0 (13).

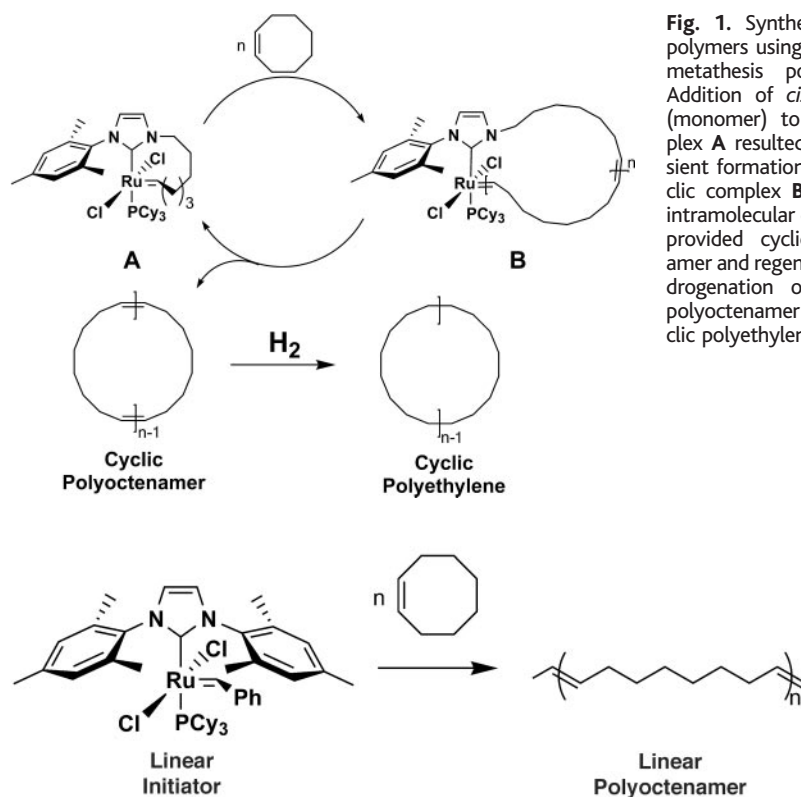
The circular structure of the prepared polyoctenamers was confirmed using a variety of characterization techniques. For comparison, a series of linear polyoctenamers with similar molecular weights and PDIs were synthesized using previously reported procedures (Scheme 1). Size-exclusion chromatography (SEC) (Fig. 2, A and B) indicated that the physically more compact cyclic polymers possessed smaller hydrodynamic volumes (i.e., they eluted later) and had lower intrinsic viscosities than their linear analogs ($[\eta]_{cyclic}/[\eta]_{linear} = 0.4$) (14). Furthermore, Mark-Houwink plots ($\log \eta$ versus $\log M_w$) (Fig. 2B) ruled out the possibility that these effects were related to conformational differences, as both polymers appeared to behave as random coils in solution (the Mark-Houwink parameter was 0.7 in both cases). The root mean square (RMS) radius ($\langle R_g^2 \rangle^{0.5}$) of the cyclic and linear polymers was measured using SEC coupled to a multiangle

light-scattering detector. The corresponding ratio $\langle R_g^2 \rangle_{cyclic}/\langle R_g^2 \rangle_{linear}$ was found to be approximately 0.5 over a wide range of molecular weights, as predicted by theory (15) (Fig. 2C). End groups were not observable in the nuclear magnetic resonance (NMR) spectra in any of the isolated cyclic polymers (16), and signals in the mass spectrum [obtained using a matrix-assisted laser desorption ionization–time of flight (MALDI-TOF) mass spectrometer] were multiples of 110.2 (C_8H_{12}) with a remainder equal only to the matrix ion.

Although these characterization techniques provided strong physical evidence for circularity of the polymers synthesized, additional proof was obtained from chemical methods as well. Substrates containing 1,2-diols are known to undergo carbon-carbon bond cleavage to produce the corresponding bis-carboxylic acid species upon addition of excess Jones's Reagent (CrO_3/H_2SO_4) (17). Linear (MW = 35 kD; PDI = 1.8) and cyclic (MW = 9 kD; PDI = 1.9) polyoctenamers containing on average only one 1,2-diol group per polymer chain were obtained by adding a small amount of 1,2-diol-5-cyclooctene during the ROMP of *cis*-cyclooctene (18). After the cyclic and linear polyoctenamers were independently reacted with Jones's Reagent, the resultant polymers were precipitated from excess acetone and collected. Cleaving the 1,2-diol containing

cyclic polyoctenamer afforded a polymer with a similar polydispersity but a larger apparent molecular weight (14 kD versus 9 kD) (Fig. 3). The increased molecular weight was expected because linear polymers have larger hydrodynamic volumes than their cyclic analogs. In contrast, the polymer obtained by cleaving the linear polyoctenamer showed not only an apparent molecular weight that was nearly cut in half (MW = 19 kD; PDI = 2.3) but one that was more polydisperse as well (19).

Hydrogenation of the isolated cyclic polyoctenamers afforded the corresponding cyclic polyethylenes (20). Differential scanning calorimetry (DSC) was used to compare the thermal properties of high molecular weight (MW \approx 200 kD) cyclic polyethylene with a linear analog of similar molecular weight (Fig. 2D). The cyclic polymer had a slightly higher melting point ($T_m = 132^\circ C$) and crystallization point ($T_c = 115^\circ C$) when compared with its linear analog ($T_m = 130^\circ C$; $T_c = 113^\circ C$). Because the enthalpy of fusion was found to be identical for both samples ($\Delta H_f \approx 100$ J/mol K), the difference appears to be related to the increased disorder (entropy) of the linear polymer. When equal amounts of linear and cyclic polyethylenes were mixed and melted together ($200^\circ C$) and then slowly cooled ($1^\circ C/min$ to $25^\circ C$) and annealed ($150^\circ C$, 36 hours), their characteristic T_m and T_c points were again observed



Scheme 1.

Fig. 1. Synthesis of cyclic polymers using ring-opening metathesis polymerization. Addition of *cis*-cyclooctene (monomer) to cyclic complex **A** resulted in the transient formation of macrocyclic complex **B**. Subsequent intramolecular chain transfer provided cyclic polyoctenamer and regenerated **A**. Hydrogenation of the cyclic polyoctenamer afforded cyclic polyethylene.

upon subsequent thermal cycling. However, when equal amounts of the two samples were dissolved in hot xylenes followed by rapid

solvent evaporation, depressed melting and crystallization points ($T_m = 127^\circ\text{C}$; $T_c = 110^\circ\text{C}$) were observed. We believe that the

low mobility of the high molecular weight chains caused by polymer entanglement and/or threading prevented phase separation even under prolonged annealing. These two observations suggest that the cyclic and linear polyethylenes are not phase compatible, and in the latter experiment they were effectively behaving as contaminants to each other. For comparison, phase separation is known to occur in mixtures of linear and highly branched (>8 branches/100 backbone carbons) polyethylene (21).

We postulated that the lack of end groups could also influence surface topology. Thin films of low molecular weight cyclic and linear polyethylenes ($M_w \approx 10$ kD) were cast from xylenes, and their interfacial contact angle with water was measured following literature methods (22). The film composed of the cyclic polymer showed a larger contact angle ($\theta = 105 \pm 2^\circ$) than its linear analog ($\theta = 96 \pm 2^\circ$), which indicated that the interface with water was smaller on the cyclic polymer's surface. Migration of the linear polymer's end groups to the surface would be expected to form a different interfacial topology than the cyclic polymer and thus may lead to contact angle hysteresis (23).

In summary, we report a strategy for the synthesis of cyclic polymers that circumvents the need for linear precursors and low concentrations, which have been limiting factors in traditional approaches. A metal complex was designed to effectively hold the ends of growing polymer chains together while catalyzing the continued addition of monomer. The foundation of the technique is based on Ru-mediated ring-opening metathesis polymerization, which is intrinsically mild and robust and permits easy access to large quantities of polymers with tunable molecular weights. As a demonstration of the versatility and potential utility of this strategy, cyclic polyethylenes, which have remained elusive despite polyethylene's ubiquity, were synthesized and found to display physical properties in solution, in bulk, and at the interface such that they were distinct from chemically identical linear analogs.

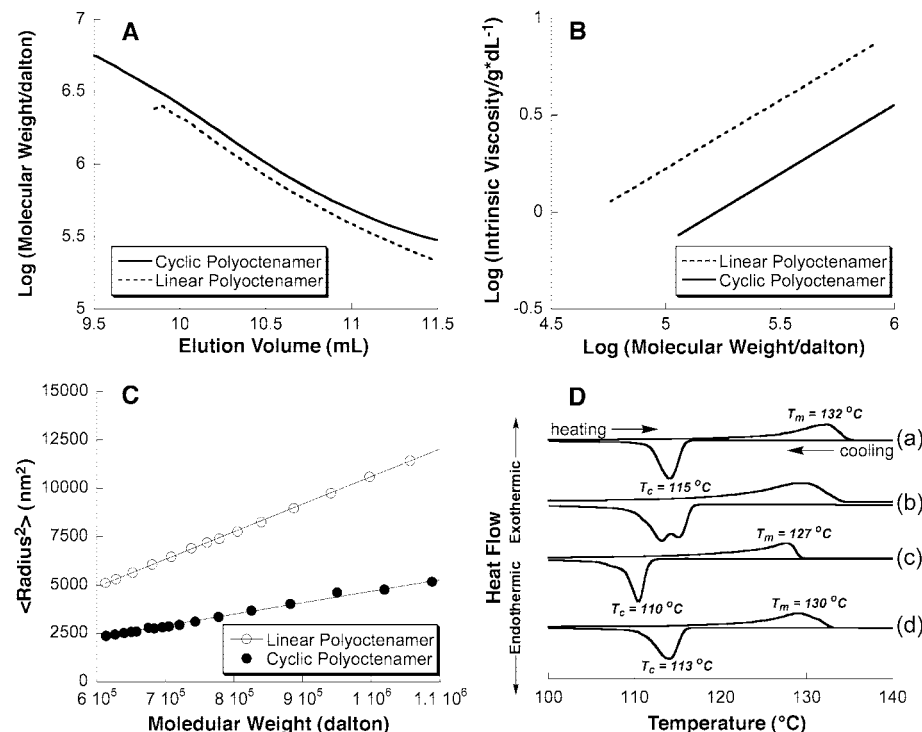


Fig. 2. Comparison of the physical properties of the cyclic and linear polymers prepared in this work. (A) Plot of elution volume versus molecular weight (eluent = THF; the reported molecular weights were determined by light-scattering methods and are therefore considered absolute). (B) Plot of log η versus log M_w (Mark-Houwink plot). (C) Plot of the mean square radius ($\langle R^2 \rangle$) versus molecular weight. (D) Differential scanning calorimetry thermograms: (a) cyclic polyethylene, $M_n \approx 200$ kD; (b) an equal mixture of cyclic and linear polyethylene after they were melted (200°C), cooled to 25°C , and then annealed for 36 hours; (c) an equal mixture of cyclic and linear polyethylene, previously dissolved in xylenes, after solvent was removed; (d) linear polyethylene, $M_n \approx 200$ kD. In all cases, the heating and cooling rates were $10^\circ\text{C}/\text{min}$, and the analyses were performed under an atmosphere of nitrogen.

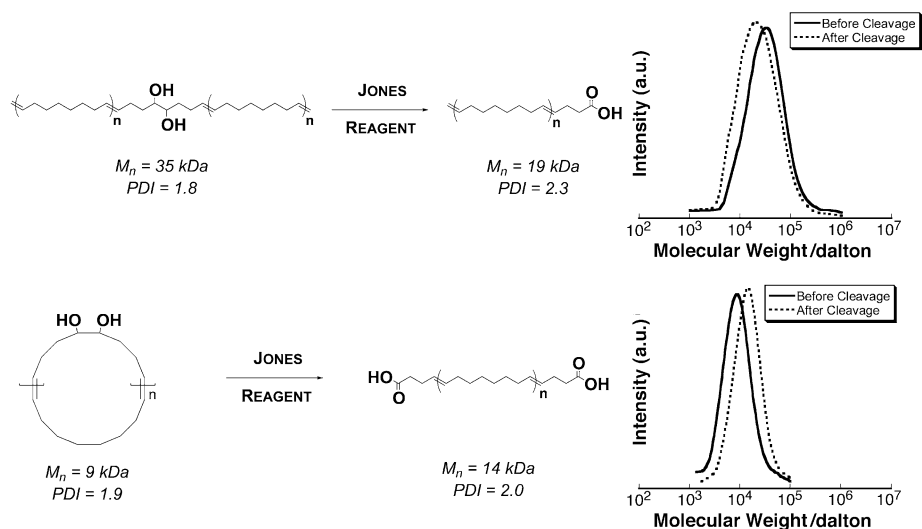


Fig. 3. Cleavage experiments that aided in distinguishing between cyclic and linear polymers. Linear (top) and cyclic (bottom) polyoctenamers containing, on average, only one 1,2-diol unit per polymer chain were synthesized. Each polymer was separately reacted with Jones's Reagent ($\text{CrO}_3/\text{H}_2\text{SO}_4$), which selectively cleaved the 1,2-diol into the corresponding bis-carboxylic acids. The molecular weight and PDI information listed above was obtained from the SEC chromatograms shown directly to the right of each example.

References and Notes

1. A. J. Peacock, *Handbook of Polyethylene: Structure, Properties, and Applications* (Marcel Dekker, New York, 2000).
2. J. A. Semlyen, *Cyclic Polymers* (Kluwer Academic, Dordrecht, The Netherlands, ed. 2, 2000).
3. W. Lee et al., *Macromolecules* **35**, 529 (2002), and references therein.
4. H. Höcker, K. Riebel, *Makromol. Chem.* **178**, 3101 (1977).
5. K. S. Lee, G. Wegner, *Makromol. Chem.-Rapid* **6**, 203 (1985).
6. Shea and co-workers [K. J. Shea, S. Y. Lee, B. B. Busch, *J. Org. Chem.* **63**, 5746 (1998)] reported a similar approach to functionalized cyclic polyethylenes using "polyhomologation." However, their strategy uses acyclic monomers, and only low molecular weight boron containing polymers were reported.
7. K. J. Ivin, J. C. Mol, *Olefin Metathesis and Metathesis Polymerization* (Academic Press, San Diego, 1997).

8. For a review of the development of Ru-based olefin metathesis catalysts, see [T. Trnka, R. H. Grubbs, *Acc. Chem. Res.* **34**, 18 (2001)].
9. A. Fürstner *et al.*, *Chem. Eur. J.* **7**, 3236 (2001).
10. Over 80% of complex **A** can be recovered from the polymerization by column chromatography (neutral silica gel, pentane/diethyl ether as eluent).
11. The presence of even small amounts of acyclic olefins leads to linear polymer contamination. For example, linear polymer was observed when attempts were made at synthesizing cyclic polybutadiene from 1,5-cyclooctadiene, which contains approximately 0.1% of 5-vinylcyclohexene as an impurity.
12. When initial monomer concentrations of less than 0.2 M were used, only low molecular cyclic oligomers (MW < 2 kD) were obtained. The result is probably related to the critical monomer concentration of *cis*-cyclooctene (~0.25 M in toluene).
13. Olefin metathesis polymerization with extensive chain transfer approximates a step-growth polymerization where polymers with PDIs = 2.0 are expected. Chain transfer is known to occur during metathesis polymerizations when catalyzed by Ru complexes ligated with *N*-heterocyclic carbenes [C. W. Bielawski, R. H. Grubbs, *Angew. Chem. Int. Ed.* **39**, 2903 (2000)].
14. Viscosity measurements were performed in tetrahydrofuran (THF) at 30°C using a SEC-viscometer apparatus. The observed ratio of 0.4 is in accord with theory for cyclic and linear polymers in good solvents [W. Burchard, in *Cyclic Polymers* (Elsevier Applied Science, London, 1986), pp. 43–84].
15. B. H. Zimm, W. H. Stockmayer, *J. Chem. Phys.* **17**, 1301 (1949).
16. The geometry of the olefins in polymer backbone was determined to be predominantly *trans* (~66%).
17. K. B. Wiberg, *Oxidation in Organic Chemistry* (Academic Press, New York, 1965).
18. $[1,2\text{-diol-5-cyclooctene}]_0/[cis\text{-cyclooctene}]_0 = 25$; $[total\ monomer]_0 = 0.5\ M\ in\ CH_2Cl_2$.
19. By assuming a continuous and random distribution of cleavable groups into infinitely long chains, the PDI was calculated to increase by a factor of 4/3 after cleavage.
20. The cyclic polyoctenamers were hydrogenated using either standard $H_2/Pd/C$ procedures or tosylhydrazine decomposition [S. F. Hahn, *J. Polym. Sci. Polym. Chem.* **30**, 397 (1992)]. Either procedure resulted in hydrogenation of more than 99% of the olefins in the polyoctenamer's backbone, as determined by 1H and ^{13}C NMR spectroscopy.
21. G. D. Wignall *et al.*, *Macromolecules* **33**, 551 (2000), and references therein.
22. D. Y. Kwok, A. W. Neumann, *Adv. Colloid Interface Sci.* **81**, 167 (1999).
23. No differences in θ were observed between high molecular weight (~200 kD) cyclic and linear polyoctenamers. This supports our belief that surface topology is affected by the presence (or absence) of end groups.
24. Financial support from the National Science Foundation (NSF) is gratefully acknowledged. We thank W. H. Stockmayer (Dartmouth College) for valuable discussions. We are indebted to M. Chen and S. Podzimek (Wyatt Technology Corporation, Santa Barbara, CA) for assistance with Wyatt's light-scattering equipment. C.B. is grateful to the NSF and the American Chemical Society Division of Organic Chemistry for predoctoral fellowships.

24 June 2002; accepted 8 August 2002

Buffered Tree Population Changes in a Quaternary Refugium: Evolutionary Implications

P. C. Tzedakis,^{1*} I. T. Lawson,² M. R. Frogley,³ G. M. Hewitt,⁴ R. C. Preece⁵

A high-resolution pollen record from western Greece shows that the amplitude of millennial-scale oscillations in tree abundance during the last glacial period was subdued, with temperate tree populations surviving throughout the interval. This provides evidence for the existence of an area of relative ecological stability, reflecting the influence of continued moisture availability and varied topography. Long-term buffering of populations from climatic extremes, together with genetic isolation at such refugial sites, may have allowed lineage divergence to proceed through the Quaternary. Such ecologically stable areas may be critical not only for the long-term survival of species, but also for the emergence of new ones.

The Pleistocene refugium hypothesis (1) proposed that population fragmentation during individual glacial stages of the Quaternary promoted speciation. A more recent view is that the accentuated environmental instability did not lead to increased speciation rates, with most species predating the Pleistocene (2, 3). This evolutionary stability has been attributed to orbital (2) and millennial (4) climate fluctuations, which undo microevolutionary changes by forcing repeated population crashes, range shifts, and gene flow. Central to this view is that the alternation of

climate phases does not generally allow sufficient time for genetic differentiation to species rank. However, molecular genetic data reveal considerable divergence between populations of many species in southern refugial centers in Iberia, Italy, the Balkans, and Greece, which took several glacial-interglacial cycles to accumulate (5–7). Analysis of DNA divergence in animals (6, 8) shows that species have continued forming through the Pleistocene and that such divergence has proceeded apparently unhindered in some places (7, 9). DNA divergence indicates that, whereas in lowland tropical forests most species formed before the Quaternary, clusters of recently diverged lineages along with older species are found in tropical mountain regions (10, 11). It has thus been postulated (10) that these mountains are centers for speciation because they provide a relatively stable habitat through climate oscillations in which older species survive and new lineages are generated. Although little paleoecological evidence has been available, this long-term stability is thought to be a function of con-

tinued moisture availability and varied topography (7, 10). A revised view of Quaternary evolutionary trends is that, while climate variability mostly inhibited speciation, species continued to form in places where presumed ecological stability allowed accumulation of genetic divergence over several glacial-interglacial cycles.

Here we present a new pollen record from a refugial site in Greece and test the extent to which certain habitats in mid-latitude areas remained immune from the extreme effects of Quaternary climate variability. The Ioannina basin (Fig. 1) is an intramontane plateau, 470 m above sea level (a.s.l.), situated in a topographically diverse landscape on the western flank of the Pindus mountain range, where the presence of refugial tree populations has been previously documented (12). The basin has a sub-Mediterranean climate with high annual precipitation [mean January temperature (T_{jan}) 4.9°C; mean July temperature (T_{jul}) 24.9°C; annual precipitation (p_{ann}) 1200 mm]. Core I-284 (39°45'N, 20°51'E; 319 m length) was drilled in 1989 near the previously studied I-249 site (12). An initial age model for I-284 (13) has here been modified by using calibrated radiocarbon ages for the last 21,000 ^{14}C years and an astronomical calibration of certain vegetation patterns for the rest of the sequence (14). Results of pollen analysis (14) from the upper 102 m of the I-284 core, spanning the past 130,000 years, are presented in Figs. 2 and 3B; mean sampling interval is ~225 years, 10 times as fine as the interval in I-249, and higher than other comparable European pollen sequences.

Three broad vegetation types are represented by the palynological assemblages of I-284: (i) forest communities [arboreal pollen (AP) > 70%] during the Last Interglacial [111.8 to 127.3 thousand calendar years ago (ka)], Interstadial 1 (88 to 104.5 ka), Interstadial 2 (68 to 83 ka) and the early Holocene (5 to 11.5 ka); (ii) communities of intermediate forest cover (70% > AP > 40%) during the Middle Pleni-

¹School of Geography, University of Leeds, Leeds, LS2 9JT, UK. ²Godwin Institute for Quaternary Research, Department of Geography, University of Cambridge, Downing Place, Cambridge, CB2 3EN, UK. ³Centre for Environmental Research, School of Chemistry, Physics and Environmental Science, University of Sussex, Falmer, Brighton, BN1 9QJ, UK. ⁴School of Biological Sciences, University of East Anglia, Norwich NR4 7TJ, UK. ⁵Godwin Institute for Quaternary Research, Department of Zoology, University of Cambridge, Downing Street, Cambridge, CB2 3EJ, UK.

*To whom correspondence should be addressed. E-mail P.Tzedakis@geog.leeds.ac.uk